Autonomous Motorcycles for Agile Maneuvers, Part II: Control Systems Design

Jingang Yi, Yizhai Zhang, and Dezhen Song

Abstract— **In this paper, we present trajectory tracking and balancing of autonomous motorcycles for agile maneuvers. Based on the newly developed autonomous motorcycle dynamics in the companion paper, we present a nonlinear control design. The control systems design is based on the external/internal convertible (EIC) dynamical structure of the motorcycle dynamics. The control design of the EIC systems guarantees an exponential convergence of the motorcycle trajectory to a neighborhood of the desired profiles while the roll motion converges to a neighborhood of the desired equilibria that are estimated under a given desired trajectory. The effectiveness of the integrated control systems are demonstrated and validated by two numerical examples based on a racing motorcycle prototype.**

I. Introduction

In our companion paper [1], we presented a new dynamic model of autonomous motorcycles for agile maneuvers. The new features of the dynamic model in [1] are the relaxation of the zero lateral velocity nonholonomic constraint of the wheel contact points and the inclusion of the tire/road friction models. The control input variables of the motorcycle dynamic model are the front wheel steering angle and the angular velocities of the front and rear wheels. The objective of this paper is to develop a simultaneous trajectory tracking and balancing control system using the developed motorcycle model in [1].

Control of an autonomous motorcycle only using the steering and vehicle velocity as inputs is challenging due to the platform's non-minimum phase and underactuation properties [1]. For such systems, there does not exist an analytical casual compensator for *exactly* output tracking while keeping the internal stability [4]. With an extra rider lean as an control input, it has been shown that maneuvering a bicycle becomes easier because adding the extra control input essentially eliminates the right half-plane zeros [5]. In [6], an autonomous bicycle is designed and balanced using gyroscopic actuators. The controller in [6] is based on a linearized bicycle model. In [7], a nonlinear control method is designed for a trajectory tracking and balancing. In [8], a balancing and tracking control mechanism is designed by on-board shifting weights. In [9], [10], a simplified inverted pendulum model is utilized for bicycle balancing. A proportional derivative (PD) controller with a disturbance observer is employed to balance the bicycle. The authors however focus on balancing the bicycle on a straight-line motion.

In this paper, we employ and extend the control design in [7], [11]. In [7], an external/internal convertible (EIC) dynamical system is presented and the motorcycle dynamics are of an example of the EIC systems. A nonlinear tracking control design is also discussed for the non-minimum phase bicycle dynamic systems. In our previous work [11], we have extended the dynamic models to consider motorcycle geometric and steering mechanism properties. In [7], [11], nonholonomic constraints of zero lateral velocity at the rear wheel contact point are enforced and only rear wheel friction force is considered for traction/braking forces. In our companion paper [1], we relax the nonholonomic constraints assumptions and consider that both wheels can produce braking actuation though the traction is only from the rear wheel. Because of the additional control input in the new model, the EIC model-based control design is presented in this paper. Indeed, the control systems design takes advantages of the control actuation flexibility and reduces the design complexity than those in [7], [11]. Two simulation examples demonstrate the effectiveness and efficacy of the control systems design.

The remainder of the paper is organized as follows. In Section II, we first review the motorcycle dynamics in [1] and then present an EIC-based tracking and balancing control design. Simulation results are presented in Section III. Finally, we conclude the paper and the future research directions in Section IV.

II. Control Systems Design

A. Motorcycle dynamics

The motorcycle dynamics with tire models are obtained in [1] as follows.

$$\mathbf{M}(\boldsymbol{q},\sigma)\ddot{\boldsymbol{q}} = \mathbf{K}(\dot{\boldsymbol{q}},\boldsymbol{q},\sigma) + \mathbf{B}\boldsymbol{u}, \tag{1}$$

where state variables $\dot{\boldsymbol{q}} := [\dot{\varphi} \quad v_{rx} \quad v_{ry}]^T$ denote the generalized velocity of the motorcycle, control input $\boldsymbol{u} := \begin{bmatrix}\omega_\sigma & \boldsymbol{u}_\lambda^T\end{bmatrix}^T$, $\boldsymbol{u}_\lambda = \begin{bmatrix}\lambda_{fs} & \lambda_{rs}\end{bmatrix}^T$, where ω_σ is the steering angular velocity, λ_{fs} and λ_{rs} are the front and rear tire slips,

This work is supported in part by the National Science Foundation under grant CMMI-0856095.

J. Yi is with the Department of Mechanical and Aerospace Engineering, Rutgers University, Piscataway, NJ 08854 USA. E-mail: jgyi@rutgers.edu.

Y. Zhang is with the Department of Information and Communication Engineering, Xi'an Jiaotong University, Xi'an 710049, Shaanxi Province, P.R. China.

D. Song is with the Department of Computer Science and Engineering, Texas A&M University, College Station, TX 77843 USA. E-mail: dzsong@cse.tamu.edu.

[1] An underactuated mechanical system is referred to a mechanical dynamic system in which the number of control inputs is less than the number of the generalized coordinates [2]. Readers can also refer to [3] for an overview of control of nonlinear non-minimum phase systems.

Preprint submitted to 48th IEEE Conference on Decision and Control.
Received March 5, 2009.

respectively. Matrices $\mathbf{M}$, $\mathbf{K}$, and $\mathbf{B}$ are functions of state variables and details of these matrices and variables are given in [1].

B. External/Internal convertible dynamical systems

The EIC form of a nonlinear dynamical system can be viewed as a special case of the normal form.

Definition 1 ([7]): A single-input, single-output, $n(=m+p)$-dimensional time-invariant nonlinear control system is called in an *external/internal convertible form* if the system is of the form

$$\Sigma(u)\begin{cases}\dot{x}_i = x_{i+1}, & i=1,\cdots,m-1,\\ \dot{x}_m = u,\\ \dot{\alpha}_i = \alpha_{i+1}, & i=1,\cdots,p-1,\\ \dot{\alpha}_p = f(x,\alpha)+g(x,\alpha)u,\\ y = x_1,\end{cases} \tag{2}$$

with input $u\in\mathbb{R}$, output $y\in\mathbb{R}$, state variables (x,α), with $x:=(x_1,\cdots,x_m)\in\mathbb{R}^m$ and $\alpha:=(\alpha_1,\cdots\alpha_p)\in\mathbb{R}^p$. The coordinates (x,α) are assumed to be defined on the open ball $\mathbf{B}_r\subset\mathbb{R}^n$ about the origin. The origin is assumed to be an equilibrium of the system, namely, $f(0,0)=0$. The functions $f(x,\alpha)$ and $g(x,\alpha)$ are C^n in their arguments, and $g(x,\alpha)\neq 0$ for all $(x,\alpha)\in\mathbf{B}_r$. Moreover, we refer to the *external subsystem* of $\Sigma(u)$ as

$$\Sigma_{\text{ext}}(u)\begin{cases}\dot{x}_i = x_{i+1}, & i=1,\cdots,m-1,\\ \dot{x}_m = u,\end{cases} \tag{3}$$

and the *internal subsystem* of $\Sigma(u)$ as

$$\Sigma_{\text{int}}(u)\begin{cases}\dot{\alpha}_i = \alpha_{i+1}, & i=1,\cdots,p-1,\\ \dot{\alpha}_p = f(x,\alpha)+g(x,\alpha)u.\end{cases} \tag{4}$$

Fig. 1 shows the structure of an EIC system. An EIC system is *convertible* because under a simple state-dependent input and an output transformation, the internal system is converted to an external system, and the external system is converted to an internal system (*dual* structure). To see such a property, let

$$u = g(x,\alpha)^{-1}\left[v - f(x,\alpha)\right] \tag{5}$$

define a state-dependent input transformation, $u\mapsto v$. Define $\xi=\alpha^1$ as the *dual output*. Apply transformation (5) to the EIC system (2) and the resulting system is referred to the *dual* of $\Sigma(u)$.

$$\Sigma_d(v)\begin{cases}\dot{x}_i = x_{i+1}, & i=1,\cdots,m-1,\\ \dot{x}_m = -g(x,\alpha)^{-1}f(x,\alpha)+g(x,\alpha)^{-1}v,\\ \dot{\alpha}_i = \alpha_{i+1}, & i=1,\cdots,p-1,\\ \dot{\alpha}_p = v,\\ \xi = \alpha_1.\end{cases} \tag{6}$$

Thus the use of input transformation (5) and the output assignment $\xi=\alpha_1$ converts the internal dynamics of $\Sigma(u)$ to the external dynamics of $\Sigma_d(v)$, and the external dynamics of $\Sigma(u)$ to the internal dynamics of $\Sigma_d(v)$.

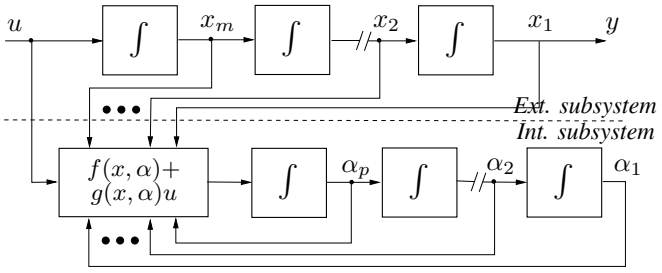

Fig. 1. An external/internal convertible system.

Since the EIC form is a special normal form of nonlinear dynamical systems, we can apply the input-output linearization method [3], [12] to convert (1) into an EIC form. Let $B_{22}\in\mathbb{R}^{2\times 2}$, $B_{22}\in\mathbb{R}^{2\times 2}$, and $K_2\in\mathbb{R}^2$ denote the block elements of matrices $\mathbf{M}$, $\mathbf{B}$, and $\mathbf{K}$, respectively [1]. Using the input transformation

$$\boldsymbol{u}_\lambda = B_{22}^{-1}M_{22}\left[M_{22}^{-1}\left(M_{21}\ddot{\varphi}-K_2-B_{21}\omega_\sigma\right)+\boldsymbol{u}_a\right], \tag{7}$$

Eq. (1) becomes

$$\begin{cases} M_{11}\ddot{\varphi} = K_1 - M_{12}\boldsymbol{u}_a + B_{11}\omega_\sigma\,,\\ \begin{bmatrix}\dot{v}_{rx}\\ \dot{v}_{ry}\end{bmatrix} = \begin{bmatrix}a_{rx}\\ a_{ry}\end{bmatrix} =: \boldsymbol{u}_a,\end{cases} \tag{8}$$

where $\boldsymbol{u}_a$ is the controlled acceleration of point C_2 in the xyz coordinate system. We also define the controlled jerk of point C_2 and yaw acceleration as

$$\boldsymbol{u}_j := \begin{bmatrix}u_{rx}\\ u_{ry}\\ u_\psi\end{bmatrix} = \begin{bmatrix}\dot{a}_{rx}\\ \dot{a}_{ry}\\ \ddot{\psi}\end{bmatrix} = \begin{bmatrix}\dot{\boldsymbol{u}}_a\\ \frac{v_{rx}\omega_\sigma+\sigma a_{rx}}{l}\end{bmatrix}, \tag{9}$$

where we use kinematics $l\dot{\psi}=\sigma v_{rx}$ in the calculation. Let (X,Y) denote the coordinates of the contact point C_2 and then we have

$$\begin{bmatrix}v_X\\ v_Y\end{bmatrix} = \begin{bmatrix}\dot{X}\\ \dot{Y}\end{bmatrix} = \begin{bmatrix}\mathrm{c}_\psi & -\mathrm{s}_\psi\\ \mathrm{s}_\psi & \mathrm{c}_\psi\end{bmatrix}\begin{bmatrix}v_{rx}\\ v_{ry}\end{bmatrix}.$$

Differentiating the above equation twice (dynamic extension), we obtain

$$\begin{bmatrix}\ddot{v}_X\\ \ddot{v}_Y\end{bmatrix} = \mathbf{U}+\boldsymbol{u}_J, \tag{10}$$

where

$$\mathbf{U} = \begin{bmatrix}-2\dot{v}_{rx}\,\mathrm{s}_\psi & -2\dot{v}_{ry}\,\mathrm{c}_\psi & -v_{rx}\dot{\psi}\,\mathrm{c}_\psi & +v_{ry}\dot{\psi}\,\mathrm{s}_\psi\\ 2\dot{v}_{rx}\,\mathrm{c}_\psi & -2\dot{v}_{ry}\,\mathrm{s}_\psi & -v_{rx}\dot{\psi}\,\mathrm{s}_\psi & -v_{ry}\dot{\psi}\,\mathrm{c}_\psi\end{bmatrix}\dot{\psi}$$

and

$$\boldsymbol{u}_J := \begin{bmatrix}\mathrm{c}_\psi & -\mathrm{s}_\psi\\ \mathrm{s}_\psi & \mathrm{c}_\psi\end{bmatrix}\begin{bmatrix}u_{rx}\\ u_{ry}\end{bmatrix} + \begin{bmatrix}-v_{rx}\,\mathrm{s}_\psi - v_{ry}\,\mathrm{c}_\psi\\ v_{rx}\,\mathrm{c}_\psi - v_{ry}\,\mathrm{s}_\psi\end{bmatrix}u_\psi. \tag{11}$$

We define the new inputs u_X and u_Y such that

$$\boldsymbol{u}_J = -\mathbf{U}+\begin{bmatrix}u_X\\ u_Y\end{bmatrix} \tag{12}$$

and then the motorcycle dynamics (8) are in the EIC form as

$$\Sigma_{\text{ext}}\begin{cases}\begin{bmatrix}\ddot{v}_X\\ \ddot{v}_Y\end{bmatrix} = \begin{bmatrix}u_X\\ u_Y\end{bmatrix},\end{cases} \tag{13a}$$

$$\Sigma_{\text{int}}\begin{cases}\ddot{\varphi} = \frac{g}{h}\left(\mathrm{s}_\varphi + \frac{bl_t\,\mathrm{c}_\xi\,\dot{\psi}}{hv_{rx}}\,\mathrm{c}_\varphi\right) - \frac{1}{h}\Big(1 - \\ \qquad \frac{h\dot{\psi}}{v_{rx}}\,\mathrm{s}_\varphi\Big)\dot{\psi}v_{rx}\,\mathrm{c}_\varphi - \frac{1}{h}\,\mathrm{c}_\varphi\,u_{\psi y},\end{cases} \tag{13b}$$

Preprint submitted to 48th IEEE Conference on Decision and Control.
Received March 5, 2009.

where

$$u_{\psi y} := b u_\psi + a_{ry}. \tag{14}$$

Remark 1: When the motorcycle runs along a straightline, $\sigma = 0$ and matrix B_{22} becomes singular and we cannot use input transformation (7). In this case, we calculate the total braking force from the second equation of the motions and split two the front and rear wheels in a way not producing any net moments around mass center G. A similar approach is discussed in [13]. If the resultant total force is traction, then it must be produced by the rear wheel.

C. Trajectory tracking control

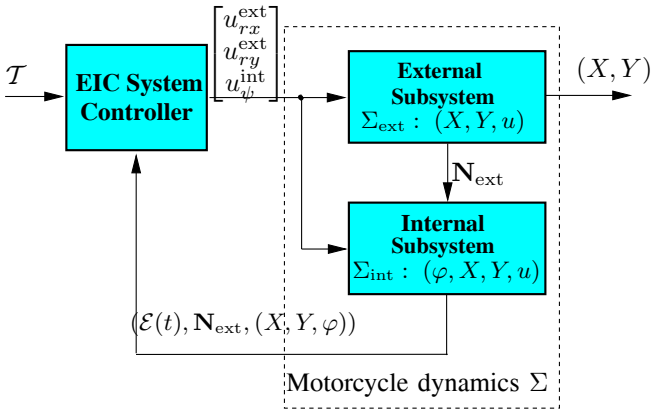

Fig. 2. EIC-based approximate output tracking control of the autonomous motorcycle dynamics.

1) Control system overview: The trajectory control system then guides the motorcycle to follow the desired trajectory $\mathcal{T}$: $(X_d(t), Y_d(t))$ while keeping the platform balanced and stable. We here employ and extend the control design approach in [7]. Fig. 2 illustrates such a control scheme.

The trajectory control design consists of two steps. The first step to design a tracking control $\mathbf{u}_{\rm ext}$ of the external subsystem $\Sigma_{\rm ext}$ for the desired trajectory $\mathcal{T}$. The second step is to design a balancing controller for the internal subsystem $\Sigma_{\rm int}$ around the internal equilibrium manifold, denoted as $\mathcal{E}(t)$. The internal equilibrium manifold $\mathcal{E}(t)$ is an embedded sub-manifold in the state space and dependent on the external control $\mathbf{u}_{\rm ext}$ and the external subsystem. Estimations of internal equilibrium and its derivatives are obtained by a dynamic inversion technique [7]. The final control system is a combination of external and internal design and is casual.

2) Approximate tracking control: We assume that the desired trajectory $\mathcal{T}: (X_d(t), Y_d(t))$ is at least C^4, namely, differentiable at least to fourth order [2]. This is feasible since the motion planning algorithm can usually generate a set of piecewise circular curves (C^∞) for $\mathcal{T}$ [14].

We design a controller $\mathbf{u}_{\rm ext}$ to track the desired trajectory $(X_d(t), Y_d(t))$ for the external subsystem $\Sigma_{\rm ext}$ (13a) disregarding, for the moment, the evolution of the internal subsystem $\Sigma_{\rm int}$ (13b).

$$\boldsymbol{u}^{\rm ext} := \begin{bmatrix} u_X^{\rm ext} \\ u_Y^{\rm ext} \end{bmatrix} = \begin{bmatrix} X_d^{(3)} \\ Y_d^{(3)} \end{bmatrix} - \sum_{i=1}^{3} b_i \begin{bmatrix} X^{(i-1)} - X_d^{(i-1)} \\ Y^{(i-1)} - Y_d^{(i-1)} \end{bmatrix}, \tag{15}$$

where the constants b_i, $i = 1, 2, 3$, are chosen such that the polynomial equation $s^3 + b_3 s^2 + b_2 s + b_1 = 0$ is Hurwitz. Under such a control, we define a nominal external vector field $\mathbf{N}_{\rm ext}$ as

$$\mathbf{N}_{\rm ext} := \begin{bmatrix} \dot{X}(t) \\ \ddot{X}(t) \\ X_d^{(3)} - \sum_{i=1}^{3} b_i \left(X^{(i-1)} - X_d^{(i-1)} \right) \\ \dot{Y}(t) \\ \ddot{Y}(t) \\ Y_d^{(3)} - \sum_{i=1}^{3} b_i \left(Y^{(i-1)} - Y_d^{(i-1)} \right) \end{bmatrix}, \tag{16}$$

By external control (15) and the input transformation (12), we find the input $\boldsymbol{u}_J^{\rm ext} = -\mathbf{U} + \boldsymbol{u}^{\rm ext}$. From (11), we obtain $\boldsymbol{u}_j^{\rm ext}$ as

$$\begin{bmatrix} u_{rx} \\ u_{ry} \end{bmatrix} + \begin{bmatrix} -v_{ry} \\ v_{rx} \end{bmatrix} u_\psi = \begin{bmatrix} \mathrm{c}_\psi & \mathrm{s}_\psi \\ -\mathrm{s}_\psi & \mathrm{c}_\psi \end{bmatrix} \boldsymbol{u}_J. \tag{17}$$

Note that $\boldsymbol{u}_J \in \mathbb{R}^2$ and $\boldsymbol{u}_j \in \mathbb{R}^3$ and the above equation is underdetermined. There are many options to determine $\boldsymbol{u}_j$ from (17). Here we propose to choose $u_\psi = \ddot{\psi} = 0$ because such a choice significantly reduces the complexity of the control design as shown in the following.

$$\boldsymbol{u}_j^{\rm ext} = \begin{bmatrix} u_{rx}^{\rm ext} \\ u_{ry}^{\rm ext} \\ u_\psi^{\rm ext} \end{bmatrix} = \begin{bmatrix} \boldsymbol{R}(\psi) \boldsymbol{u}_J^{\rm ext} \\ 0 \end{bmatrix} = \begin{bmatrix} \boldsymbol{R}(\psi) \left(-\mathbf{U} + \boldsymbol{u}^{\rm ext} \right) \\ 0 \end{bmatrix}. \tag{18}$$

Next, we consider the internal (roll angle) equilibrium, denoted as φ_e, by substituting $u_\psi^{\rm ext}$ and $u_{ry}^{\rm ext}$ above into the internal subsystem dynamics (13b). We define the implicit function F_φ of φ as

$$F_\varphi := g \left(\tan\varphi + \frac{b l_t \dot{\psi}\, \mathrm{c}_\xi}{h v_{rx}} \right) - \left(1 - \frac{h \dot{\psi}\, \mathrm{s}_\varphi}{v_{rx}} \right) \dot{\psi} v_{rx} - u_{\psi y}^{\rm ext}, \tag{19}$$

$u_{\psi y}^{\rm ext} = b u_\psi^{\rm ext} + a_{ry} = a_{ry}$, and thus the roll angle equilibrium $\varphi_e := \varphi_e(\dot{\psi}, v_{rx}, \boldsymbol{u}_j^{\rm ext})$ is a solution of the algebraic equation $F_{\varphi_e} = 0$. We define an internal (roll angle) equilibrium manifold $\mathcal{E}(t)$ as

$$\mathcal{E}(t) = \left\{ \left(X^{(0,2)}, Y^{(0,2)}, \varphi^{(0,1)} \right) \;\middle|\; \varphi = \varphi_e,\ \dot{\varphi} = 0 \right\}. \tag{20}$$

The internal equilibrium manifold $\mathcal{E}(t)$ can be viewed as a time-dependent graph over the 6-dimensional (X, Y)-subspace in $\mathbb{R}^6$ of the external subsystem (13a) that is evolved with the external nominal vector field $\mathbf{N}_{\rm ext}$ (16) under the external subsystem control $\boldsymbol{u}^{\rm ext}$.

For the motorcycle balance systems, we like to control the roll angle φ around $\mathcal{E}(t)$ while the external subsystem is tracking $\mathcal{T}$ under the control of $\boldsymbol{u}^{\rm ext}$. Note that $\dot{\varphi}_e \neq 0$ and $\ddot{\varphi}_e \neq 0$ in general and here we approximate the derivatives

[2]For the external subsystem control, we only need $\mathcal{T}$ to be C^3. The requirement for C^4 is due to the estimation of the internal (roll angle) equilibrium and its derivatives by a dynamic inversion technique.

Preprint submitted to 48th IEEE Conference on Decision and Control.
Received March 5, 2009.

$\dot{\varphi}_e$ and $\ddot{\varphi}_e$ by using directional derivatives [3], [12] along the vector field $\mathbf{N}_{\rm ext}$ due to their dependence on the external subsystems and $\boldsymbol{u}^{\rm ext}$. We define the directional derivative (or Lie derivative) as $\bar{L}_{\mathbf{N}_{\rm ext}}\varphi_e := L_{\mathbf{N}_{\rm ext}}\varphi_e + \frac{\partial \varphi_e}{\partial t}$ and $\bar{L}^2_{\mathbf{N}_{\rm ext}}\varphi_e := \bar{L}_{\mathbf{N}_{\rm ext}}\bar{L}_{\mathbf{N}_{\rm ext}}\varphi_e$. With the above approximations for $\dot{\varphi}_e$ and $\ddot{\varphi}_e$, the stabilizing control of the internal subsystem $\Sigma_{\rm int}$ (13b) around $\mathcal{E}(t)$ is then given by the following feedback linearization

$$u^{\rm int}_{\psi y} = \left(\frac{\mathrm{c}_\varphi}{h}\right)^{-1}\left[\frac{g}{h}\left(\mathrm{s}_\varphi + \frac{bl_t\,\mathrm{c}_\xi\,\dot{\psi}}{hv_{rx}}\,\mathrm{c}_\varphi\right) - \frac{1}{h}\left(1 - \frac{h\dot{\psi}}{v_{rx}}\,\mathrm{s}_\varphi\right)\dot{\psi}v_{rx}\,\mathrm{c}_\varphi - v_{\psi y}\right], \tag{21a}$$

$$v_{\psi y} = \bar{L}^2_{\mathbf{N}_{\rm ext}}\varphi_e - \sum_{i=1}^{2} a_i(\varphi^{(i-1)} - \bar{L}^{i-1}_{\mathbf{N}_{\rm ext}}\varphi_e). \tag{21b}$$

where constants a_1 and a_2 are chosen such that the polynomial equation $s^2 + a_2 s + a_1 = 0$ is Hurwitz. Therefore, the internal control is obtained from (14) as

$$u^{\rm int}_{\psi} = \frac{1}{b}\left(u^{\rm int}_{\psi y} - a_{ry}\right) \tag{22}$$

The *final* control system design of the motorcycle balance system (10) combines the above development in (22) and (18) as

$$\boldsymbol{u}_j = \begin{bmatrix} u^{\rm ext}_{rx} \\ u^{\rm ext}_{ry} \\ u^{\rm int}_{\psi} \end{bmatrix} \tag{23}$$

It is noted that the coupling between the external- and internal-subsystem control designs is through the introduction of the internal equilibrium manifold $\mathcal{E}(t)$. By defining $\mathcal{E}(t)$, we approximately decouple the external and internal subsystems due to the EIC dual structural properties of the motorcycle system.

We define $\boldsymbol{\vartheta}(t) = [X(t)\ v_X(t)\ \dot{v}_X(t)\ Y(t)\ v_Y(t)\ \dot{v}_Y(t)]^T$ as the state variables of the external subsystem and $\boldsymbol{\varrho}(t) = [\varphi(t)\ \ \dot{\varphi}(t)]^T$ as the state variables of the internal subsystem. We also define the output $\boldsymbol{\zeta}(t) = [X(t)\ Y(t)]^T$ and desired output $\boldsymbol{\zeta}_d(t) = [X_d(t)\ Y_d(t)]^T$. We assume that the desired trajectory $\boldsymbol{\zeta}_d(t)$ and its derivatives (up to the fourth order) are bounded by a positive number $\epsilon > 0$, namely, $\boldsymbol{\zeta}_d(t) \in \mathbf{B}^{(4)}_\epsilon := \{\boldsymbol{x}(t)\,|\,\|\boldsymbol{x}^{(0,4)}(t)\|_\infty < \epsilon\}$, where $\|\boldsymbol{x}^{(0,n)}(t)\|_\infty := \sup_{t\ge 0}\|\boldsymbol{x}^{(0,n)}(t)\|_\infty$. We also define the tracking errors $e^{\vartheta}_i = \boldsymbol{\vartheta}_i - X^{(i-1)}_d$, $e^{\vartheta}_{i+3} = \boldsymbol{\vartheta}_{i+3} - Y^{(i-1)}_d$, $i = 1,2,3$, $e^{\varphi}_j = \varphi^{(j)} - \varphi^{(j)}_e$, $j = 0,1$, and $\boldsymbol{e} := [e^{\vartheta}_1,\ \cdots,\ e^{\vartheta}_6,\ e^{\varphi}_1,\ e^{\varphi}_2]^T$. We also define the perturbation error p_φ $(= O(\|\boldsymbol{\zeta}^{(0,4)}_d(t)\|, \|\boldsymbol{e}\|)$ as the approximation errors by using the directional derivatives for $\dot{\varphi}_e$ and $\ddot{\varphi}_e$ in the internal subsystem control design (21b), namely,

$$p_\varphi = \bar{L}^2_{\mathbf{N}_{\rm ext}}\varphi_e - \ddot{\varphi}_e + \sum_{i=1}^{2} a_i(\varphi^{(i-1)}_e - \bar{L}^{i-1}_{\mathbf{N}_{\rm ext}}\varphi_e).$$

We similarly define another two perturbation errors p_X $(= O(\|\boldsymbol{\zeta}^{(0,4)}_d(t)\|, \|\boldsymbol{e}\|)$ and p_Y $(= O(\|\boldsymbol{\zeta}^{(0,4)}_d(t)\|, \|\boldsymbol{e}\|)$ due to the resulting errors in the external subsystem state $\boldsymbol{\vartheta}(t)$ using the internal subsystem control $u^{\rm int}_{\psi y}$ in the external subsystem (23). An explicit formulation for p_X and p_Y can be similarly found by the dual structure of EIC system [7]. We consider the perturbation vector for the error dynamics of $\Sigma(u)$ (12) under control (23) as

$$p(\boldsymbol{\zeta}^{(0,4)}_d(t), \boldsymbol{e}) = [0,\ 0,\ p_X,\ 0,\ 0,\ p_Y,\ 0,\ p_\varphi]^T.$$

We assume an affine perturbation for $p(y^{(0,4)}_d(t), e)$, namely, there exist constants $k_1 > 0$ and $k_2 > 0$ such that $\|p(\boldsymbol{\zeta}^{(0,5)}_d(t), \boldsymbol{e})\|_\infty \le k_1\epsilon + k_2\|\boldsymbol{e}\|_\infty$.

We only state the convergence properties of the approximate tracking control design in this section. The proof of these properties follows directly from Proposition 6.7.4 and Theorem 6.7.6 in [7] and we omit here.

Theorem 1: For the balance system (12), assuming that the desired trajectory $\boldsymbol{\zeta}_d(t) \in \mathbf{B}^{(4)}_\epsilon$ for some $\epsilon > 0$ and if the affine perturbation constant $k_2 > 0$ is a sufficiently small real number, then there exists a $t_1 > 0$, and a class-$\mathcal{K}$ function $r(\epsilon)$ such that for all $(\boldsymbol{e}^{\vartheta}(0), \boldsymbol{e}^{\varphi}(0)) \in \mathbf{B}_{r(\epsilon)}$, $(\boldsymbol{e}^{\vartheta}(t), \boldsymbol{e}^{\varphi}(t))$ converges to zero exponentially until $(\boldsymbol{e}^{\vartheta}(t), \boldsymbol{e}^{\varphi}(t))$ enters $\mathbf{B}_{r(\epsilon)}$. Once $(\boldsymbol{e}^{\vartheta}(t), \boldsymbol{e}^{\varphi}(t))$ enters $\mathbf{B}_{r(\epsilon)}$, it will stay in $\mathbf{B}_{r(\epsilon)}$ thereafter.

3) Estimation of the internal equilibrium: A dynamic inversion technique approach in [7] is used to estimate the internal equilibrium state φ_e in (21b). To illustrate the dynamic inversion technique, we differentiate $F_\varphi = 0$ with time, and using the fact that $u^{\rm ext}_{\psi} = \ddot{\psi} = 0$ we obtain

$$\dot{\varphi}_e = \frac{1}{g\sec^2\varphi_e + h\dot{\psi}\,\mathrm{c}_{\varphi_e}}\left(\frac{gbl_t\,\mathrm{c}_\xi\,\dot{\psi}\dot{v}_{rx}}{hv^2_{rx}} + \dot{\psi}\dot{v}_{rx} + u^{\rm ext}_{ry}\right) =: E(\varphi_e, \dot{\psi}, v_{rx}, \dot{v}_{rx}, u^{\rm ext}_{ry}). \tag{24}$$

A dynamic inverter for an estimate $\hat{\varphi}_e$ of the internal equilibrium φ_e is designed as

$$\dot{\hat{\varphi}}_e = -\beta F_{\hat{\varphi}} + E(\hat{\varphi}_e, \dot{\psi}, v_{rx}, \dot{v}_{rx}, u^{\rm ext}_{ry}), \tag{25}$$

where $F_{\hat{\varphi}_e}$ is given by (19) and $\beta > 0$ is the inverter gain. The proof of the exponential convergence of the estimation (25) follows directly from the development of the dynamic inversion technique in [7].

The estimate of the directional derivative $\bar{L}_{\mathbf{N}_{\rm ext}}\varphi_e$ in (21b) is obtained by (25), namely, $\bar{L}_{\mathbf{N}_{\rm ext}}\varphi_e = E(\varphi_e, \dot{\psi}, v_{rx}, \dot{v}_{rx}, u^{\rm ext}_{ry})$. The estimate of $\bar{L}^2_{\mathbf{N}_{\rm ext}}\varphi_e$ is obtained by directly taking one more directional derivative of $\bar{L}_{\mathbf{N}_{\rm ext}}\varphi_e$ along $\mathbf{N}_{\rm ext}$. For brevity, we give the derivation in Appendix. We also list the calculation of $\bar{L}_{\mathbf{N}_{\rm ext}}u^{\rm ext}_{rx}$ and $\bar{L}_{\mathbf{N}_{\rm ext}}u^{\rm ext}_{ry}$ in Appendix. Such calculations are needed for computing $\bar{L}^2_{\mathbf{N}_{\rm ext}}\varphi_e$. The approximation errors in estimating φ_e (by $\hat{\varphi}_e$) and its directional derivatives $\bar{L}_{\mathbf{N}_{\rm ext}}\varphi_e$ and $\bar{L}^2_{\mathbf{N}_{\rm ext}}\varphi_e$ (by $\bar{L}_{\mathbf{N}_{\rm ext}}\hat{\varphi}_e$ and $\bar{L}^2_{\mathbf{N}_{\rm ext}}\hat{\varphi}_e$, respectively) can be considered as additional terms in the perturbation $p(\boldsymbol{\zeta}^{(0,4)}_d(t), \boldsymbol{e})$. Therefore, the stability results of the approximate control design in the previous section are still held.

Remark 2: Although the above control system design is similar to those in [7], the final form is much simpler because we have chosen $u^{\rm ext}_{\psi} = 0$ in (18). We have such a flexibility by (17) to determine $\boldsymbol{u}_j$ because we have three control input variables now while in [7] only the rear wheel

Preprint submitted to 48th IEEE Conference on Decision and Control.
Received March 5, 2009.

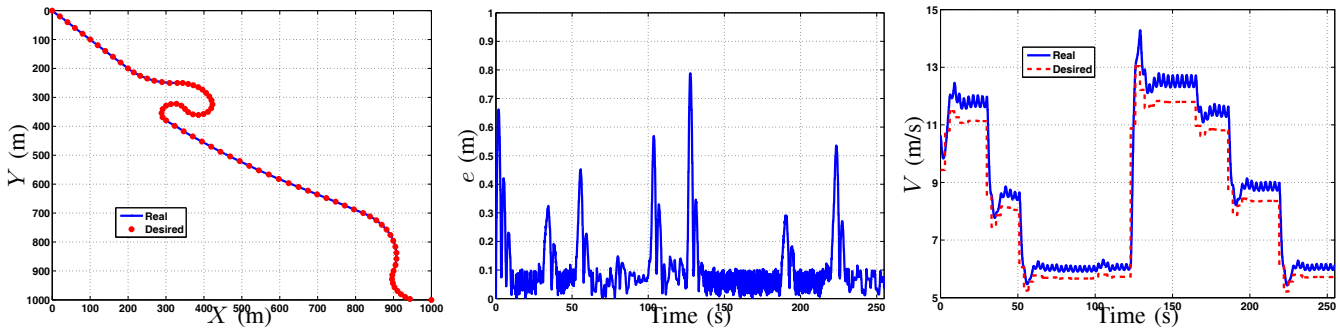

(a) (b) (c)

Fig. 3. A general trajectory tracking. (a) Trajectory positions. (b) Tracking position error. (c) Rear wheel contact point velocity magnitude.

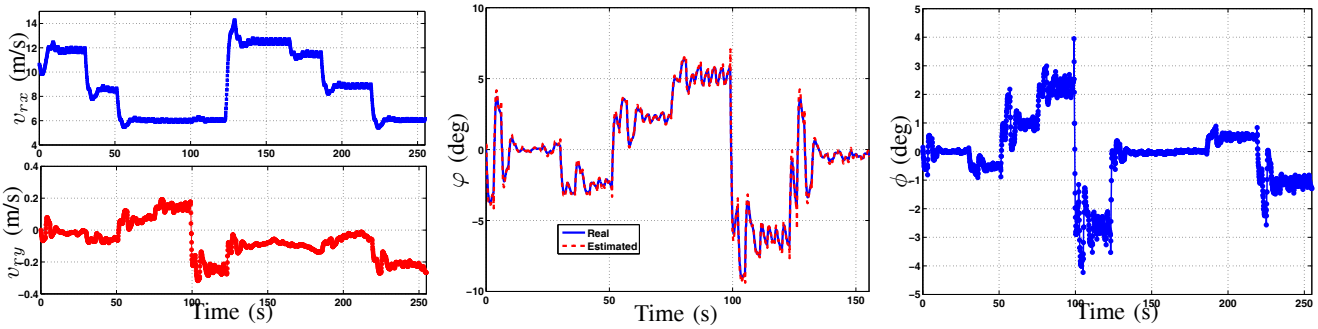

(a) (b) (c)

Fig. 4. Roll angle and steering angle of the general trajectory tracking. (a) Rear wheel contact point body-frame velocities v_{rx} and v_{ry}. (b) Roll angle φ. (b) Steering angle ϕ.

driving torque and the steering angle are controlled. Because of this difference, we only require the trajectory $\mathcal{T}$ is at least C^4 rather than C^5 as the requirement of the controller in [7]. Using optimization techniques by considering the input constraints for determining $\boldsymbol{u}_j$ by (17) is an extension of the control design and currently ongoing research.

III. Simulation Results

In this section, we demonstrate the control systems design through two numerical examples. The first example is taken from [11] for showing a general motorcycle trajectory and the second example to illustrate an aggressive maneuvers with a large side slip angles.

We use a racing motorcycle prototype in [15], [16] as the controlled motorcycle in our simulation. The motorcycle parameters are listed in Table I. We use the tire 160/70 in [15] for the racing motorcycle since the testing data are available in the paper. The tire stiffness coefficients listed in Table I are calculated under the nominal load $F_z = 1600$ N.

Fig. 3 shows the trajectory tracking performance of a general trajectory. The position errors under the control system in Fig. 3(b) are within 1 meter with the center line of the track throughout the entire course. The desired velocity in Fig. 3(c) is determined by the curvature of the trajectory. In Fig. 4, we have shown the roll angle φ, the body-frame velocities v_{rx} and v_{ry} of rear wheel contact point C_2, and steering angle ϕ. From Fig. 4(a) we clearly see that the lateral velocity v_{ry} is quite small most time because the motorcycle is running along a straight-line in most time. At turning locations, the longitudinal velocity is reduced and the lateral velocity increases. The roll angle and steering angle are small for such a small-curvature trajectory.

Fig. 5 shows the longitudinal slips and side slip angles of the front and rear wheels. Again, it is clear that the slip values at both wheels are small. The front wheel only brakes and the rear wheel generates traction or braking forces. For example, when the motorcycle accelerates around 120 s, the rear wheel slip has a large negative spike to produce the traction force. When the vehicle needs to reduce velocity, both wheels brake with a set of large positive slip spikes shown in Fig. 5(a). The side slip angles shown in Fig. 5(b) clearly illustrate that at large-curvature locations, the side slip angles are large to produce the lateral forces to turn the motorcycle. Typically, the rear side slip angles are small and close to zero.

The second example shows that the motorcycle runs under a more aggressive maneuver. The desired trajectory is "8"-shape with circular radius of 25 meters; see Fig. 6(a). In Fig. 6(a), the motorcycle starts from the origin and moves along the direction indicated by the arrows in the figure. The desired velocity of the motorcycle moving along the "8"-shape trajectory is designed to be varying significantly as shown in Fig. 6(c). Comparing with the previous example, the tracking errors of the "8"-shape trajectory are much larger; see Fig. 6(b). This is mainly due to the quick change of the desired velocity profile.

Fig. 7 shows the body-frame velocity, roll angle, and steering angle for the "8"-shape trajectory. We clearly see

Preprint submitted to 48th IEEE Conference on Decision and Control.
Received March 5, 2009.

TABLE I

MOTORCYCLE PARAMETERS

m (kg)	b (m)	l (m)	l_t (m)	h (m)	ξ (deg)	r (m)	λ_{sm}	$\lambda_{\gamma m}$ (deg)	μ_m	k_λ (N)	k_φ (N/rad)	k_γ (N)
274.2	0.81	1.37	0.15	0.62	26.1	0.3	0.1	6	3	41504	23968	1227

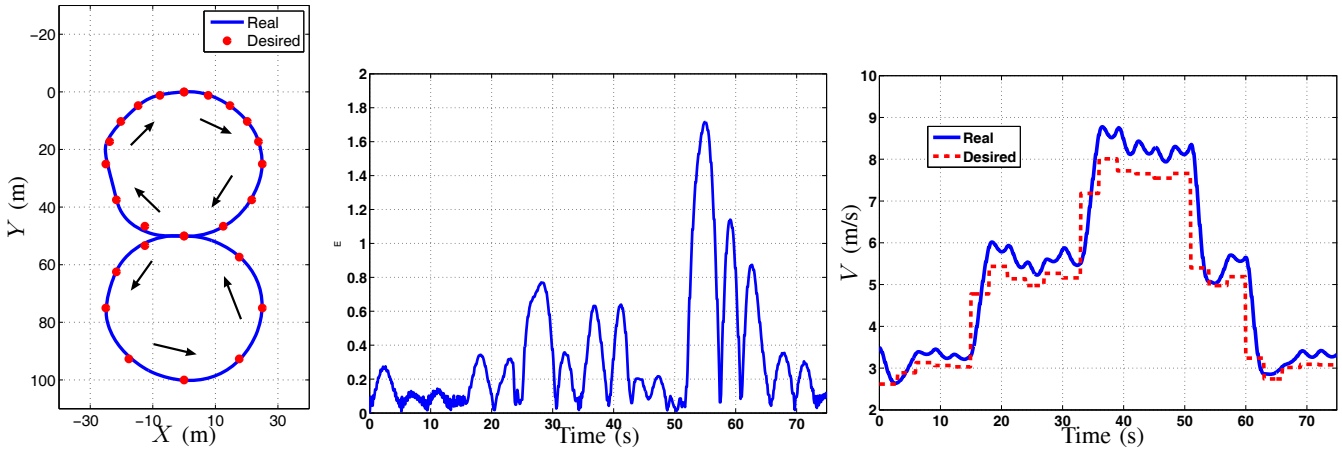

Fig. 6. An "8"-shape trajectory tracking. (a) Trajectory positions. (b) Tracking position error. (c) Rear wheel contact point velocity magnitude.

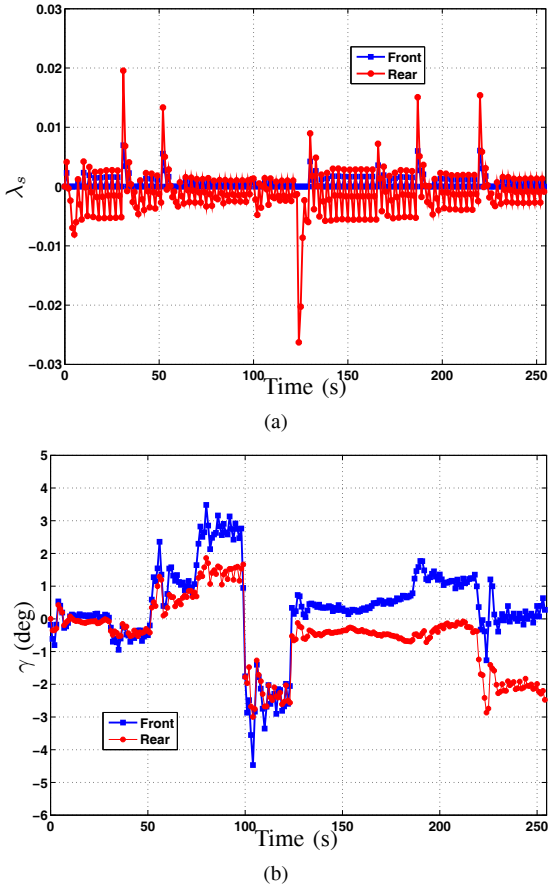

Fig. 5. Longitudinal slips and slip angles at the front and rear wheels. (a) Slip ratio λ_{fs} and λ_{rs}. (b) Slip angles γ_f and γ_r.

the change of the lateral velocity during each circle of the "8"-shape trajectory. The lateral velocity magnitude is large due to the smaller turning radius. The maximum roll angle is around 15 deg and that is much larger than that of the previous example. The steering angle is large as well to make the motorcycle turn in a tighter and small circle. The oscillations in both roll angle (Fig. 7(b)) and steering angle (Fig. 7(c)) are probably due to the variations in the desired velocity.

We clearly see a large side slip angles shown in Fig. 8(b). Particularly, for the front wheel, we have seen a 15 degree side slip angle. For the rear wheel, the side slip angle reaches almost 6 degrees, which is around the saturation point of the tire characteristics (Table I). In other words, the motorcycle rear wheel is starting to slide on the ground. If the side slip angle increases further, the stability of the motorcycle will change significantly. The longitudinal slip are relatively small since the longitudinal acceleration of the motorcycle is not large and the racing motorcycle tire is stiff. This simulation example demonstrates that the proposed dynamic model and control systems capture the realistic aggressive motorcycle maneuvers.

IV. CONCLUSION

The focus of this second-part paper is on the control systems design of autonomous motorcycles for agile maneuvers. The nonlinear control design presented in this paper take advantages of the external/internal convertible (EIC) dynamical structure of the motorcycle dynamics, and extend to the three control inputs case. Such an extension allows some flexibility in control systems design and therefore simplifies the complexity of the final calculation. We have demonstrated the control systems design through two simulation examples using a racing motorcycle prototype.

Preprint submitted to 48th IEEE Conference on Decision and Control.
Received March 5, 2009.

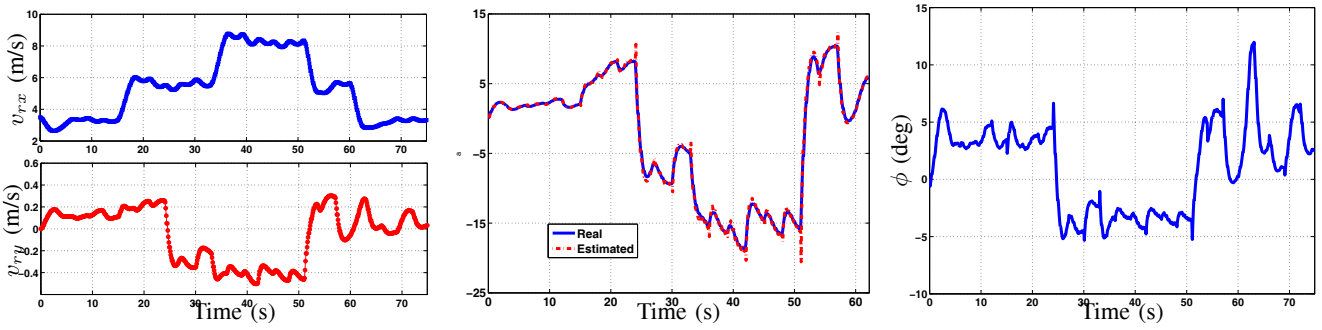

(a) (b) (c)

Fig. 7. Roll angle and steering angle of the "8"-shape trajectory tracking. (a) Rear wheel contact point body-frame velocities v_{rx} and v_{ry}. (b) Roll angle φ. (b) Steering angle ϕ.

There are several ongoing research directions. We are currently implementing the proposed control systems on a Rutgers autonomous motorcycle platform. We will report the implementation results in the near future. Moreover, we also plan to study how the professional racing drivers control motorcycles for agile maneuvers.

ACKNOWLEDGMENTS

The first author thanks Dr. N. Getz at Inversion Inc. for his helpful suggestions and support. The authors are grateful to Prof. S. Jayasuriya at Texas A&M University, Dr. E.H. Tseng and Dr. J. Lu at Ford Research and Innovation Center for their helpful discussions and suggestions.

REFERENCES

[1] J. Yi, Y. Zhang, and D. Song, "Autonomous motorcycles for agile maneuvers: Part I: Dynamic modeling," *Submitted to the 48th IEEE Conf. on Decision and Control*.

[2] F. Bullo and A. Lewis, *Geometric Control of Mechanical Systems: Modeling, Analysis, and Design for Simple Mechanical Control Systems*. New York, NY: Springer, 2004.

[3] S. Sastry, *Nonlinear Systems: Analysis, Stability, and Control*. New York, NY: Springer, 1999.

[4] J. Grizzle, M. Di Benedetto, and F. Lamnabhi-Lagarrigue, "Necessary conditions for asymptotic tracking in nonlinear systems," *IEEE Trans. Automat. Contr.*, vol. 39, no. 9, pp. 1782–1794, 1994.

[5] K. Åström, R. Klein, and A. Lennartsson, "Bicycle dynamics and control," *IEEE Control Syst. Mag.*, vol. 25, no. 4, pp. 26–47, 2005.

[6] A. Beznos and A. Formal'sky and E. Gurfinkel and D. Jicharev and A. Lensky and K. Savitsky and L. Tchesalin, "Control of autonomous motion of two-wheel bicycle with gyroscopic stabilisation," in *Proc. IEEE Int. Conf. Robot. Autom.*, Leuven, Belgium, 1998, pp. 2670–2675.

[7] N. Getz, "Dynamic inversion of nonlinear maps with applications to nonlinear control and robotics," Ph.D. dissertation, Dept. Electr. Eng. and Comp. Sci., Univ. Calif., Berkeley, CA, 1995.

[8] S. Lee and W. Ham, "Self-stabilzing strategy in tracking control of unmanned electric bicycle with mass balance," in *Proc. IEEE/RSJ Int. Conf. Intell. Robot. Syst.*, Lausanne, Switzerland, 2002, pp. 2200–2205.

[9] Y. Tanaka and T. Murakami, "Self sustaining bicycle robot with steering controller," in *Proc. 2004 IEEE Adv. Motion Contr. Conf.*, Kawasaki, Japan, 2004, pp. 193–197.

[10] ——, "A study on straight-line tracking and posture control in electric bicycle," *IEEE Trans. Ind. Electron.*, vol. 56, no. 1, pp. 159–168, 2009.

[11] J. Yi, D. Song, A. Levandowski, and S. Jayasuriya, "Trajectory tracking and balance stabilization control of autonomous motorcycles," in *Proc. IEEE Int. Conf. Robot. Autom.*, Orlando, FL, 2006, pp. 2583–2589.

[12] A. Isidori, *Nonlinear Control Systems*, 3rd ed. London, UK: Springer-Verlag, 1995.

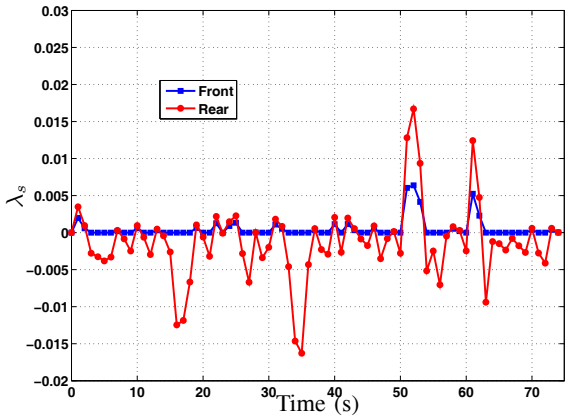

(a)

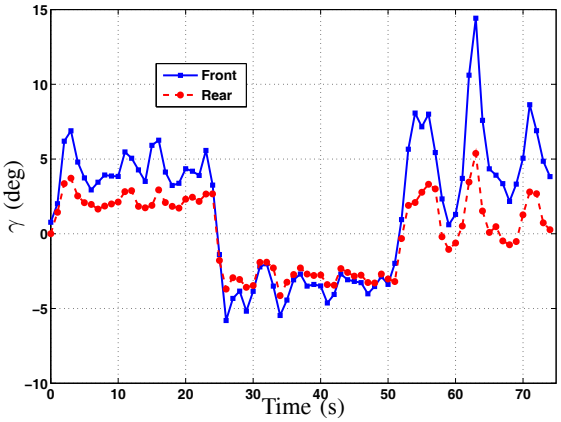

(b)

Fig. 8. Longitudinal slips and slip angles at the front and rear wheels of the "8"-shape trajectory tracking. (a) Slip ratio λ_{fs} and λ_{rs}. (b) Slip angles γ_f and γ_r.

[13] J. C. Gerdes and E. J. Rossetter, "A unified approach to driver assistance systems based on artificial potential fields," *ASME J. Dyn. Syst., Meas., Control*, vol. 123, no. 3, pp. 431–438, 2001.

[14] D. Song, H.-L. Lee, J. Yi, and A. Levandowski, "Vision-based motion planning for an autonomous motorcycle on ill-structured roads," *Autonomous Robots*, vol. 23, no. 3, pp. 197–212, 2007.

[15] R. S. Sharp, S. Evangelou, and D. J. N. Limbeer, "Advances in the modelling of motorcycle dynamics," *Multibody Syst. Dyn.*, vol. 12, pp. 251–283, 2004.

[16] M. Corno, S. M. Savaresi, M. Tanelli, and L. Fabbri, "On optimal motorcycle braking," *Contr. Eng. Pract.*, vol. 16, pp. 644–657, 2008.

$$\bar{L}_{\mathbf{N}_{\text{ext}}} u_{rx}^{\text{ext}} = \begin{bmatrix} -\mathrm{s}_\psi & \mathrm{c}_\psi \end{bmatrix} \dot{\psi} \left(-\mathbf{U} + \boldsymbol{u}^{\text{ext}} \right) + \begin{bmatrix} \mathrm{c}_\psi & \mathrm{s}_\psi \end{bmatrix} \left(- \begin{bmatrix} -2u_{rx}^{\text{ext}} \mathrm{s}_\psi - 2u_{ry}^{\text{ext}} \mathrm{c}_\psi - 3\dot{v}_{rx}\dot{\psi}\, \mathrm{c}_\psi + 3\dot{v}_{ry}\dot{\psi}\, \mathrm{s}_\psi + \ddot{\psi} \left(v_{rx}\, \mathrm{s}_\psi + v_{ry}\, \mathrm{c}_\psi \right) \\ 2u_{rx}^{\text{ext}} \mathrm{c}_\psi - 2u_{ry}^{\text{ext}} \mathrm{s}_\psi - 3\dot{v}_{rx}\dot{\psi}\, \mathrm{s}_\psi - 3\dot{v}_{ry}\dot{\psi}\, \mathrm{c}_\psi - \ddot{\psi} \left(v_{rx}\, \mathrm{c}_\psi - v_{ry}\, \mathrm{s}_\psi \right) \end{bmatrix} \dot{\psi} + \begin{bmatrix} \bar{L}_{\mathbf{N}_{\text{ext}}} u_X^{\text{ext}} \\ \bar{L}_{\mathbf{N}_{\text{ext}}} u_Y^{\text{ext}} \end{bmatrix} \right)$$
$$= \dot{v}_{rx}\dot{\psi}^2 + \left(2u_{ry}^{\text{ext}} - u_X^{\text{ext}}\, \mathrm{s}_\psi + u_Y^{\text{ext}}\, \mathrm{c}_\psi \right) \dot{\psi} + \bar{L}_{\mathbf{N}_{\text{ext}}} u_X^{\text{ext}}\, \mathrm{c}_\psi + \bar{L}_{\mathbf{N}_{\text{ext}}} u_Y^{\text{ext}}\, \mathrm{s}_\psi, \tag{26}$$

$$\bar{L}_{\mathbf{N}_{\text{ext}}} u_{ry}^{\text{ext}} = \dot{v}_{ry}\dot{\psi}^2 - \left(2u_{rx}^{\text{ext}} + u_X^{\text{ext}}\, \mathrm{c}_\psi + u_Y^{\text{ext}}\, \mathrm{s}_\psi \right) \dot{\psi} - \bar{L}_{\mathbf{N}_{\text{ext}}} u_X^{\text{ext}}\, \mathrm{s}_\psi + \bar{L}_{\mathbf{N}_{\text{ext}}} u_Y^{\text{ext}}\, \mathrm{c}_\psi\,. \tag{27}$$

APPENDIX

The calculation of $\bar{L}_{\mathbf{N}_{\text{ext}}} u_{rx}^{\text{ext}}$ and $\bar{L}_{\mathbf{N}_{\text{ext}}} u_{ry}^{\text{ext}}$ is obtained by taking the Lie derivative along the nominal external vector field (16) and the control input (18). The calculation are shown in (26) and (27) on the top of this page. In these equations, we have

$$\begin{bmatrix} \bar{L}_{\mathbf{N}_{\text{ext}}} u_X^{\text{ext}} \\ \bar{L}_{\mathbf{N}_{\text{ext}}} u_Y^{\text{ext}} \end{bmatrix} = \begin{bmatrix} X_d^{(4)}(t) \\ Y_d^{(4)}(t) \end{bmatrix} - b_3 \begin{bmatrix} u_X^{\text{ext}} - X_d^{(3)}(t) \\ u_Y^{\text{ext}} - Y_d^{(3)}(t) \end{bmatrix} - \sum_{i=1}^{2} b_i \begin{bmatrix} X^{(i)} - X_d^{(i)}(t) \\ Y^{(i)} - Y_d^{(i)}(t) \end{bmatrix}.$$

Similarly, we can calculate $\bar{L}^2_{\mathbf{N}^{\text{ext}}} \varphi_e$ by directly taking a directional derivative of $\bar{L}_{\mathbf{N}_{\text{ext}}} \varphi_e$ along the vector field $\mathbf{N}_{\text{ext}}$. From (24), we have

$$\bar{L}^2_{\mathbf{N}_{\text{ext}}} \varphi_e = \left(h\dot{\psi}\, \mathrm{c}_{\varphi_e} + g \sec^2 \varphi_e \right)^{-1} \left[\frac{g b l_t\, \mathrm{c}_\xi}{h} \left(\frac{\dot{\psi} u_{rx}^{\text{ext}}}{v_{rx}^2} - \frac{2\dot{v}_{rx}^2 \dot{\psi}}{v_{rx}^3} \right) + \dot{\psi} u_{rx}^{\text{ext}} + \bar{L}_{\mathbf{N}_{\text{ext}}} u_{ry}^{\text{ext}} + \left(h\dot{\psi}\, \mathrm{s}_{\varphi_e} - 2g \sec^2 \varphi_e \tan \varphi_e \right) \left(\bar{L}_{\mathbf{N}_{\text{ext}}} \varphi_e \right)^2 \right]. \tag{28}$$

Preprint submitted to 48th IEEE Conference on Decision and Control.
Received March 5, 2009.